Continental-scale impacts of intra-seasonal rainfall variability on simulated ecosystem responses in Africa

Kaiyu Guan[1,2*], Stephen P. Good[3], Kelly K. Caylor[1], Hisashi Sato[4], Eric F. Wood[1], and Haibin Li[5]

[1]Department of Civil and Environmental Engineering, Princeton University, Princeton, NJ, USA

[2]Department of Environmental & Earth System Science, Stanford University, Stanford, CA 94025, USA

[3]Department of Geology and Geophysics, University of Utah, Salt Lake City, UT 84112, USA

[4]Graduate School of Environmental Studies, Nagoya University, D2-1(510) Furo-cho, Chikusa-ku, Nagoya-city, Aichi 464-8601, Japan

[5]Department of Earth and Planetary Sciences, Rutgers University, Piscataway, NJ 08854, USA

[*]Corresponding author:
Kaiyu Guan
Department of Environmental & Earth System Science,
Stanford University, Stanford, CA 94025, USA
Phone: 609-647-1368, Fax: 650-498-5099
Email: kaiyug@stanford.edu

Running title: Ecological Impacts of Intra-Seasonal Rainfall Variability

Submitted to *Biogeosciences*

Abstract:

Climate change is expected to modify intra-seasonal rainfall variability, arising from shifts in rainfall frequency, intensity and seasonality. These intra-seasonal changes are likely to have important ecological impacts on terrestrial ecosystems. Yet, quantifying these impacts across biomes and large climate gradients is largely missing. This gap hinders our ability to better predict ecosystem services and their responses to climate change, esp. for arid and semi-arid ecosystems. Here we use a synthetic weather generator and an independently validated vegetation dynamic model (SEIB-DGVM) to virtually conduct a series of "rainfall manipulation experiments" to study how changes in the intra-seasonal rainfall variability affect continent-scale ecosystem responses across Africa. We generated different rainfall scenarios with fixed total annual rainfall but shifts in: i) frequency vs. intensity, ii) rainy season length vs. frequency, iii) intensity vs. rainy season length. These scenarios were fed into SEIB-DGVM to investigate changes in biome distributions and ecosystem productivity. We find a loss of ecosystem productivity with increased rainfall frequency and decreased intensity at very low rainfall regimes (<400 mm/year) and low frequency (<0.3 event/day); beyond these very dry regimes, most ecosystems benefit from increasing frequency and decreasing intensity, except in the wet tropics (>1800 mm/year) where radiation limitation prevents further productivity gains. This result reconciles seemingly contradictory findings in previous field studies on rainfall frequency/intensity impacts on ecosystem productivity. We also find that changes in rainy season length can yield more dramatic ecosystem responses compared with similar percentage changes in rainfall frequency or intensity, with the largest impacts in semi-arid woodlands. This study demonstrates that not all rainfall regimes are ecologically equivalent, and that intra-seasonal rainfall characteristics play a significant role in influencing ecosystem function and structure through controls on ecohydrological processes. Our results also suggest that shifts in rainfall seasonality have potentially large impacts on terrestrial ecosystems, and these understudied impacts should be explicitly examined in future studies of climate impacts.

Keywords: rainfall frequency, rainfall intensity, rainfall seasonality, biome

distribution, Gross Primary Production (GPP), Africa

1. Introduction

Due to increased water holding capacity in the atmosphere as a consequence of global warming (O'Gorman and Schneider, 2009), rainfall is projected to change in intensity and frequency across much of the world (Easterling et al., 2000; Trenberth et al., 2003; Chou et al., 2013), in conjunction with complex shifts in rainfall seasonality (Feng et al., 2013; Seth et al., 2013). These changes possibly indicate a large increase in the frequency of extreme events and variability in rainfall (Easterling et al., 2000; Allan and Soden, 2008), and many of these changes may be accompanied with little changes in total annual rainfall (Knapp et al., 2002; Franz et al., 2010). Meanwhile, regions sharing similar mean climate state may have very different intra-seasonal variabilities, and the ecological significance of intra-seasonal climate variabilities has been largely overlooked previously in terrestrial biogeography (Good and Caylor, 2011). For example, ecosystems in West Africa and Southwest Africa (Figure 1) share similar total annual rainfall, but West Africa has much more intense rainfall events within a much shorter rainy season, while Southwest Africa has a longer and less intense rainy season. The same amount of total rainfall can come in very different ways, which may cause distinctive ecosystem responses and structure. Understanding the impacts of these regional differences in intra-seasonal rainfall variability and their possible future changes on terrestrial ecosystems is critical for maintaining ecosystem services and planning adaptation and mitigation strategies for ecological and social benefits (Anderegg et al., 2013).

[insert Figure 1]

The changes in intra-seasonal rainfall characteristics, specifically frequency, intensity and seasonality, have critical significance to ecosystem productivity and structure (Porporato et al., 2001; Weltzin et al., 2003; Williams and Albertson, 2006; Good and Caylor, 2011; Guan et al., 2014), but previous studies on this topic

(summarized in Table 1) have their limitations in the following aspects. First, existing relevant field studies mostly focus on a single ecosystem, *i.e.* grasslands, and subsequently only low rainfall regimes have been examined to date (mostly below 800mm/year, see Table 1). Grasslands have the largest sensitivity to hydrological variabilities among all natural ecosystems (Scanlon et al., 2005; Guan et al., 2012), however inferences drawn from a single ecosystem are limited in scope and difficult to apply to other ecosystems. Second, even within grasslands, different studies have seemingly contradictory findings (see Table 1), and there is a lack of a comprehensive framework to resolve these inconsistencies. Specifically, whether increased rainfall intensity with decreased rainfall frequency has positive (Knapp et al., 2002; Fay et al., 2003; Robertson et al., 2009; Heisler-White et al., 2009) or negative impacts (Heisler-White et al., 2009; Thomey et al., 2011) on grassland productivity is still under debate. Third, previous relevant studies mostly focus on the impacts of rainfall frequency and intensity (Table 1 and Rodríguez-Iturbe and Porporato, 2004), and largely overlook the possible changes in rainfall seasonality (here rainy season length in particular). Rainfall frequency and intensity mostly describe rainfall characteristics within the rainy season, but do not account for the impacts of interplay between rainy season length and dry season length (Guan et al., 2014). For ecosystems predominately controlled by water availability, rainy season length constrains the temporal niche for active plant physiological activities (van Schaik et al., 1993; Scholes and Archer, 1997), and large variations in rainfall seasonality can lead to significant shifts in biome distribution found from paleoclimate pollen records (e.g. Vincens et al., 2007). Given changes in rainfall seasonality have been found in various tropical regions (Feng et al., 2013) and have been projected in future climate (Biasutti and Sobel, 2009; Shongwe et al., 2009; Seth et al., 2013), studies investigating their impacts on terrestrial ecosystems are relatively rare, and very few field studies are designed to address this aspect (Table 1, Bates et al., 2006; Svejcar et al., 2003; Chou et al., 2008). Finally, there is an increasing trend of large-scale studies addressing rainfall variability and ecological responses using satellite remote sensing (Fang et al., 2005; Zhang et al., 2005; Good and Caylor, 2011; Zhang et al., 2013; Holmgren et al.,

2013) and flux network data (Ross et al., 2012). These large-scale studies are able to expand analyses to more types of ecosystems and different climate conditions, and provide valuable observation-based insights. However there are very few theoretical modeling works to corroborate this effort. All these above issues call for a comprehensive modeling study to investigate different aspects of intra-seasonal rainfall variability on terrestrial ecosystems spanning large environmental gradients and various biomes.

In this paper, we aim to study ecological impacts of intra-seasonal rainfall variability on terrestrial ecosystems. In particular, we design virtual "rainfall manipulation experiments" to concurrently shift intra-seasonal rainfall characteristics without changing total annual rainfall. We focus on the impacts of these different rainfall scenarios on ecosystem productivity (e.g. Gross Primary Production, GPP) and biome distributions in the African continent, simulated by an independently validated dynamic vegetation model SEIB-DGVM (Sato and Ise, 2012). Previous modeling approaches in this topic (Gerten et al., 2008; Hély et al., 2006) designed various rainfall scenarios by rearranging (halving, doubling or shifting) the rainfall amount based on the existing rainfall observations. In contrast to these approaches, we design a weather generator which is based on a stochastic rainfall model (Rodríguez-Iturbe et al., 1999), but also explicitly incorporate wet/dry season. This weather generator thus allows us to implement a series of experiments by synthetically varying two of the three rainfall characteristics (rainfall intensity, rainfall frequency, and rainy season length) while fixing total annual rainfall at the current climatology. We choose Africa as our test-bed mostly because the following two reasons: (1) the rainfall regimes and biomes have large gradients varying from extremely dry grasslands to highly humid tropical evergreen forests; (2) Africa is a continent usually assumed to have few temperature constrains (Nemani et al., 2003), which will help to isolate the impacts of precipitation from temperature, as one challenge in attributing climatic controls on temperate ecosystems or Mediterranean ecosystems is the superimposed influences from both temperature and precipitation. The overarching science question we will address is: **How do African ecosystems**

respond to possible changes in intra-seasonal rainfall variability (i.e. rainfall frequency, intensity and rainy season length)?

[insert Table 1]

2. Materials and Methods

2.1 Methodology overview

Table 1 summarizes previous field-based rainfall manipulation experiments, such as the one that Knapp et al. (2002) did in a grassland that concurrently increasing rainfall frequency and decreasing rainfall intensity while fixing total rainfall. The central idea of our study is to design similar rainfall manipulation experiments but test them virtually in the model domain across large environment gradients. We manipulate rainfall changes through a weather generator based on a parsimonious stochastic rainfall model (Rodriguez-Iturbe et al., 1984). We model the total amount of rainfall during rainy season as a product of the three intra-seasonal rainfall characteristics for the rainy season, rainfall frequency (λ, event/day), rainfall intensity (α, mm/event), and rainy season length (T_w, days) (More details in section 2.3). Thus it is possible to simultaneously perturb two of the rainfall characteristics away from their climatological values while preserving the mean annual precipitation (MAP) unchanged. We then feed these different rainfall scenarios into a well-validated dynamic vegetation model (SEIB-DGVM, section 2.2) to study simulated ecosystem responses. Detailed experiments design is described in section 2.5.

2.2 SEIB-DGVM model and its performances in Africa

We use a well-validated vegetation dynamic model SEIB-DGVM (Sato et al., 2007) as the tool to study ecosystem responses to different rainfall variabilities. This model follows the traditional "gap model" concept (Shugart, 1998) to explicitly simulate the dynamics of ecosystem structure and function for individual plants at a set of virtual vegetation patches, and uses results at these virtual patches as a surrogate to represent large-scale ecosystem states. Thus individual trees are simulated from establishment,

competition with other plants, to death, which creates "gaps" for other plants to occupy and develop. SEIB-DGVM includes mechanical-based and empirical-based algorithms for land physical processes, plant physiological processes, and plant dynamic processes. SEIB-DGVM contains algorithms that explicitly involve the mechanisms of plant-related water stress (Figure 2; Sato and Ise, 2012). With similar concepts to previous studies (e.g. Milly, 1992; Porporato et al., 2001), the current SEIB-DGVM implements a continuous "water stress factor" (Equation 2) based on the soil moisture status (Equation 1), scaling from 0 (most stressful) to 1 (with no stress), which then acts to scale the stomatal conductance for plant transpiration and carbon assimilation.

$$stat_{water} = (S - S_w) / (S_f - S_w) \quad \text{(Equation 1)}$$

$$\text{Water stress factor} = 2*stat_{water} - stat_{water}^2 \quad \text{(Equation 2)}$$

where S, S_w and S_f refer to the fraction of volumetric soil water content within the rooting depth, at the wilting point, and at field capacity, respectively. Figure 2 provides a schematic diagram of "water stress factor" from the SEIB-DGVM, and we also include an approximated linear model that has been widely adopted elsewhere (e.g. Milly, 1992; Porporato et al., 2001). The linear model uses an extra variable S*, so called "critical point" of soil moisture: when S>S*, there is no water stress (water stress factor =1); and when S<S*, water stress factor linearly decreases with the decrease of S. Though SEIB-DGVM adopts a quadratic form for "water stress factor", it essentially functions similarly as the linear model, such that S* distinguishes two soil moisture regimes that below which there is a large sensitivity of water stress to soil moisture status, and above which there is little water stress. Understanding how this "water stress factor" functions is the key to explain the following results.

[insert Figure 2]

SEIB-DGVM allows development of annual and perennial grasses as well as multiple life cycles of grass at one year based on environmental conditions. Multiple life cycles of tree growth per year are possible in theory but rarely happen in simulations (Sato

and Ise, 2012). Soil moisture status is the predominant factor to determine LAI of the vegetation layer, which influences maximum daily productivity and leaf phenology. When LAI exceeds 0 for 7 continuous days, dormant phase of perennial vegetation layer changes into growth phase. While when LAI falls below 0 for 7 continuous days, growth phase switches to dormant phase (Sato et al, 2007). SEIB-DGVM also explicitly simulates light conditions and light competition among different PFTs in the landscape based on its simulated 3D canopy structure and radiative transfer scheme (Sato et al, 2007).

SEIB-DGVM has been tested both globally (Sato et al., 2007) and regionally for various ecosystems (Sato et al., 2010; Sato, 2009; Sato and Ise, 2012), whose simulated results compare favorably with ground observations and satellite remote sensing measures for ecosystem composition, structure and function. In particular, SEIB-DGVM has been successfully validated and demonstrated its ability in simulating ecosystem structure and function in the African continent (Sato and Ise, 2012). Two plant function types (PFTs) of tropical woody species are simulated by SEIB-DGVM in Africa: tropical evergreen trees and tropical deciduous trees. The distribution of these two woody types in the simulation is largely determined by hydro-climatic environments. Tropical evergreen trees only develop in regions where water resources are sufficient all year around, so they can maintain leaves for all seasons; otherwise, tropical deciduous trees could survive and dominate the landscape as they can shed leaves if there is no sufficient water supply in its root zone during the dry season (Sato and Ise, 2012). Trees and grasses coexist in a cell, with the floor of a virtual forest monopolized by one of the two grass PFTs, C_3 or C_4 grass. The dominating grass type is determined at the end of each year by air temperature, precipitation, and CO_2 partial pressure (Sato and Ise, 2012).

SEIB-DGVM was run at 1 °spatial resolution and at the daily step. It was spun-up for 2000 years driven by the observed climate (1970-2000) repeatedly for the soil carbon pool to reach steady state, followed by 200 years simulation driven by the forcings based on the experiment design in Section 2.4. Because our purpose is to understand the direct impacts of intra-seasonal rainfall variability, we turned off the

fire component of SEIB-DGVM to exclude fire-mediated feedbacks in the results. Though we are fully aware of the important role of fire in interacting with rainfall seasonality and their influence on African ecosystems (Bond et al., 2005; Lehmann et al., 2011; Staver et al., 2012), studying these interactions is beyond the scope of this work. For the similar reason, we fixed the atmospheric CO_2 concentration at 380 ppmv to exclude possible impacts of CO_2 fertilization effects.

2.3 Synthetic weather generator

The synthetic weather generator used here has two major components: i) to stochastically generate daily rainfall based on a stochastic rainfall model, and ii) to conditionally sample all other environmental variables from historical records to preserve the covariance among climate forcing variables.

The stochastic rainfall model can be expressed as $MAP=\alpha \lambda T_w / f_w$, and we set f_w to be 0.9, i.e. the period including 90% of total annual rainfall is defined as "rainy season" (exchangeable with "wet season" hereafter). In particular, we first use Markham (1970)'s approach to find the center of the rainy season, and then extend the same length to both sides of the center until the total rainfall amount in this temporal window (i.e. "rainy season") is equal to 90% of the total annual rainfall. Rainy season and dry season have their own rainfall frequency and intensity. Two seasons are separately modeled based on the Market Poisson Process. Here we only focus on and manipulate rainy-season rainfall characteristics in our study, as rainy-season rainfall accounts for almost all the meaningful rainfall inputs for plant use. Thus in the following paper, whenever we mention α or λ, we refer to those during the rainy season.

In this rainfall model, any day can be either rainy or not, and a rainy day is counted as one rainy event; rainfall events occur as a Poisson Process, with the parameter $1/\lambda$ (unit: days/event) being the mean intervals between rainfall events, and rainfall intensity α for each rainfall event following an exponential distribution, with α being the mean rainfall intensity per event (Rodr ́guez-Iturbe et al., 1999). The wet season length is modeled as a beta distribution bounded from 0 to 1, scaled by 365

days. All the necessary parameters to fit for the stochastic rainfall model (including the mean and variance of rainfall frequency, intensity and length of wet and dry seasons) were derived from the satellite-gauge-merged rainfall measurement from TRMM 3b42V7 (Huffman et al., 2007) for the period of 1998 to 2012, based on the above assumptions for the rainfall process. Specifically, we applied our definition of "rainy season" to each year of the TRMM rainfall data for per pixel, and calculated the mean and variance of the "rainy season length", using which we fitted the beta distribution for T_w. For rainfall frequency and intensity, we lumped all the wet or dry season rainfall record together to derive their parameters. The two steps of the synthetic weather generator are described below:

Step 1: Model the daily rainfall following the Marked Poisson process described above. In particular, for a specific year, we first stochastically generate the wet season length by sampling from the beta distribution, and the dry season length is determined accordingly. Then we generate the daily rainfall for wet and dry season respectively.

Step 2: Based on the simulated daily rainfall time series in Step 1, we conditionally sample temperature, wind, and humidity from the Global Meteorological Forcing Dataset (GMFD, Sheffield et al., 2006), as well as cloud fraction and soil temperature from the Climate Forecast System Reanalysis (CFSR) from National Centers for Environmental Prediction (NCEP) (Saha et al., 2010). To sample for a specific day, all the historical record within a 21-day time window centered at that specific day makes up a sampling pool. From the sampling pool, we choose the day such that the historical rainfall amount of the chosen day is within (100-30)% to (100+30)% of the simulated daily rainfall amount. We then draw all the environmental variables (except rainfall) on that sampled day to the new climate forcing. If we can find a sample from the pool based on the above rule, this sampling is called "successful". When there is more than one suitable sample, we randomly select one. When there is no suitable sample, we randomly select one day within the pool. The mean "successful" rate for all the experiments and ensembles across Africa is 83%.

To test the validity of the synthetic weather generator, we ran SEIB-DGVM using the historical climate record ($S_{climatology}$) and the synthetic forcing ($S_{control}$), with the

latter generated using the weather generator based on the rainfall characteristics derived from the former. Figure S1 shows that the SEIB-DGVM simulations driven by these two different forcings generate similar biome distributions with a Cohen's Kappa coefficient of 0.78 (Cohen, 1960), and similar GPP patterns in Africa, with the linear fit of annual GPP as: $GPP(S_{control}) = 1.03 \times GPP(S_{climatology}) + 0.215$ ($R^2=0.89$, $P<0.0001$, Figure S2). Both biome and GPP patterns are consistent with observations (Sato and Ise, 2012). These results provide confidence in using the synthetic weather generator and SEIB-DGVM to conduct the further study.

2.4 Experiment design

Three experiments are designed as follows:

Exp 1 (Perturbation of rainfall frequency and intensity, termed as $S_{\lambda-\alpha}$ hereafter) Simulations forced by the synthetic forcings with varying λ and α simultaneously for wet season (20% increases of λ and corresponding decreases of α to make MAP unchanged; 20% decreases of λ and corresponding increases of α to make MAP unchanged; no change for dry season rainfall characteristics), while fixing T_w at the current climatology;

Exp 2 (Perturbation of rainfall frequency and rainy season length, termed as $S_{Tw-\lambda}$) Simulations forced by the synthetic forcing with varying T_w and λ simultaneously for wet season (20% increases of T_w and corresponding decreases of λ to make MAP unchanged; 20% decreases of T_w and corresponding increases of λ to make MAP unchanged; no change for dry season characteristics), while fixing α at the current climatology;

Exp 3 (Perturbation of rainy season length and intensity, termed as $S_{Tw-\alpha}$) Simulations forced by the synthetic forcing with varying T_w and α simultaneously for wet season (20% increases of T_w and corresponding decreases of α to make MAP unchanged; 20% decreases of T_w and corresponding increases of α to make MAP unchanged; no change for dry season characteristics), while fixing λ at the current climatology.

Because λ and T_w have bounded ranges (λ~[0, 1] and T_w~[0, 365]), if these two variables after perturbation exceeds the range, we would force their value to be the

lower or upper bound, and rearrange the other corresponding rainfall characteristic to ensure MAP unchanged. Each rainfall scenario has six ensemble realizations of synthetic climate forcings to account for the stochasticity of our synthetic weather generator.

3. Results

We present the differences in simulated biome distributions of the three experiments (i.e. $S_{\lambda-\alpha}$, $S_{Tw-\lambda}$, $S_{Tw-\alpha}$) in Figure 3, and their spatial patterns are shown in Figure S3 and S4. Differences in simulated annually averaged soil moisture and GPP for each experiment are shown in Figure 4 and 6. These differences represent the simulated ecosystem sensitivity to the slight perturbation of intra-seasonal rainfall characteristics deviating from the current climatology. To further explore how MAP and these rainfall characteristics affect the simulated GPP, Figure 5 shows the difference of simulated GPP as a function of MAP and a perturbed rainfall characteristic in the corresponding experiment. We term Figure 5 as "GPP sensitivity space", and "positive GPP sensitivity" means that GPP changes at the same direction with MAP or rainfall characteristics, and vise versa for "negative GPP response". These "GPP sensitivity spaces" are generated based on the aggregated mean GPP in each bin of the rainfall properties. The bin size for MAP, rainfall frequency, rainfall intensity and rainy season length are 100 mm/year, 0.05 event/day, 1 mm/event and 15 days respectively. We also provide the standard error (SE) of the "GPP sensitivity spaces" in each bin to assess their uncertainties, with higher SE meaning larger uncertainties. $SE = \sigma / \sqrt{n}$, where σ and n refer to the standard deviation of GPP values and the sample size in each bin respectively. A series of illustrations in Figure 6 were generalized from the simulated time series, and are used to explain the underlying mechanisms.

[insert Figure 3; Figure 4; Figure 5]

3.1 Ecosystem sensitivity to rainfall frequency and intensity (Experiment $S_{\lambda-\alpha}$)

Experiment $S_{\lambda-\alpha}$ assesses ecosystem responses after increasing rainfall frequency λ and decreasing rainfall intensity α (λ↑, α↓) under a fixed total annual rainfall. The simulated biome distributions show that a small portion of regions are converted from woodland to grassland at low rainfall regime (~500 mm/year), corresponding to a decrease of GPP in these regions. In the high rainfall regime (around 1500 mm/year, Figure 3a), increasing rainfall frequency significantly converts tropical evergreen forests into woodlands. In the intermediate rainfall regime (600-1000 mm/year), there is little change in biome distributions. We further check the spatial patterns of differences in annual mean soil moisture and annual total GPP (Figure 4a and 5b). We find that GPP increases with increasing rainfall frequency across most of the Africa continent, except in the very dry end (in the southern and eastern Africa) and the very wet regions (in central Africa and northeastern Madagascar). This GPP pattern mostly mirrors the soil moisture change in woodlands and grasslands (Figure 4b), except the wet tropics, where the changes of soil moisture and GPP are reversed.

Figure 5a shows the GPP sensitivity as a function of MAP and the climatological rainfall frequency, and we find three major patterns:

Pattern 1.1: Negative GPP sensitivity shows up in the very dry end of MAP regime (MAP<400 mm/year) and with relatively low rainfall frequency (λ<0.3 event/day), i.e. GPP decreases with more frequent but less intense rainfall in this low rainfall range.

Pattern 1.2: Across most rainfall ranges (MAP from 400 mm/year to 1600 mm/year), increasing frequency of rainfall (and simultaneously decreasing rainfall intensity) lead to positive GPP sensitivity. This positive GPP sensitivity peaks at the low range of rainfall frequency (~0.35 event/day) and around the MAP of 1000 mm/year.

Pattern 1.3: At the high range of MAP (>1800 mm/year) with low rainfall frequency (~0.4 event/day), GPP decreases with increased rainfall frequency.

The GPP sensitivity with respect to MAP and rainfall intensity (Fig. 6c) shows an unclear pattern, and also contains relatively large uncertainties. These large uncertainties arise mostly because the rainfall intensity of all the modeled regions cluster in a relatively narrow range (Fig. A4c), and meanwhile the simulated GPP sensitivity for these regions also have large variance (Fig. A4d). Thus we will not

388 over-interpret the pattern in Fig. 6c.

389 Pattern 1.1 and Pattern 1.2 can be explained by the illustrative time series in
390 Figure 6a and 6b, respectively. Figure 6a shows that when rainfall events are small
391 and very infrequent, increasing rainfall frequency while decreasing intensity would
392 cause more frequent downcrossings of soil moisture at the wilting point S_w, which
393 subsequently would reduce the effective time of carbon assimilation and plant growth
394 (i.e. when soil moisture is below S_w, plants would be in the extreme water stress and
395 slow down or stop physiological activity). This case only happens where MAP is very
396 low with low frequency and the biome is predominantly grasslands, which explains
397 why negative changes in soil moisture and GPP in Figure 4a and 4b are distributed in
398 those regions. This result also corroborates the field findings of the negative impacts
399 from increasing rainfall frequency in Heisler-White et al.(2009) and Thomey et al.
400 (2011) at low rainfall regimes.

401 Figure 6b provides the hydrological mechanism for the positive sensitivity of soil
402 moisture and GPP with increasing rainfall frequency over the most African continent
403 (Pattern 1.2). Once individual rainfall event has enough intensity and rainfall
404 frequency is enough, downcrossings of S_w would not easily happen. Instead, the
405 accumulative rainy-season soil moisture becomes the dominant control of plant
406 growth, and increasing rainfall frequency has led to a significant increase of soil
407 moisture for plant water use (Figure 4a and 4b). This conclusion drawn from our
408 numerical modeling is consistent with previous findings in Rodr ́guez-Iturbe and
409 Porporato (2004) based on stochastic modeling. We also find that this positive GPP
410 sensitivity reaches to its maximum in the intermediate total rainfall (~1000 mm/year)
411 and relatively low rainfall frequency (~0.35 event/day), indicating that in these
412 regimes increasing rainfall frequency could most effectively increase soil moisture for
413 plant water use and create marginal benefits of GPP to the increased rainfall frequency.
414 Further increase in large total annual rainfall or rainfall frequency would reduce the
415 sensitivity to water stress with fewer downcrossings of soil moisture critical point S*;
416 and once the soil moisture is always ample (i.e. above S*), the changes in either MAP
417 or rainfall frequency would not alter plant water stress.

Pattern 1.3 also shows a negative GPP sensitivity, but its mechanism is different from the previous case of Pattern 1.1. In regions with total rainfall usually more than 1800 mm/year, SEIB-simulated tropical forests exhibit radiation-limitation rather than water-limitation during wet season. Increase of rainfall frequency at daily scale would enhance cloud fraction and suppress plant productivity in these regions (Graham et al., 2003). Thus even though soil moisture still increases (Figure 4a), GPP decreases with increased rainfall frequency. This mechanism also explains why tropical evergreen forests shrink its area with increased rainfall frequency (Figure 3a).

It is worth noting that the magnitude of GPP changes due to rainfall frequency and intensity is relatively small in most of the woodlands, but can be relatively large for drylands with MAP below 600 mm/year (up to 10-20% of annual GPP). This pattern also explains why only modest changes in biome distribution happen between woodlands and grasslands in $S_{\lambda-\alpha}$ (Figure 3a).

[insert Figure 6]

3.2 Ecosystem sensitivity to rainfall seasonality and frequency (Experiment $S_{Tw-\lambda}$)

Experiment $S_{Tw-\lambda}$ assesses ecosystem responses after increasing rainy season length and decreasing rainfall frequency (i.e. $T_w\uparrow$, $\lambda\downarrow$) under a fixed total annual rainfall. The simulated biome distribution shows a gain of area in tropical evergreen forests converted from woodlands. The northern Africa has an area increase of woodlands converted from grasslands, and African Horn region has a small expansion of grasslands into woodlands (Figure 3b). Figure 4c and 4d show that increasing rainy season length T_w and decreasing frequency λ would significantly increase annual mean soil moisture and GPP (up to 30%) in most woodland area. Meanwhile decreased soil moisture and GPP are found in the southern and eastern Africa. Tropical evergreen forests show little response. We further explore the GPP sensitivity space in Figure 5e and 5g, and find the following robust patterns (based on small standard errors shown in Figure 5f and 5h):

Pattern 2.1: The negative GPP sensitivity tends to happen where MAP is mostly

below 1000 mm/year with long rainy season length (T_w>150 days) and low rainfall frequency (λ<0.35 event/day).

Pattern 2.2: When MAP and rainfall frequency are large enough (MAP>1000 mm/year and λ>0.4 event/day), decreasing λ while increasing T_w would significantly increase GPP. The maximum positive GPP sensitivity happens at the intermediate MAP range (1100-1500 mm/year) and the high rainfall frequency (λ~0.7 event/day).

Pattern 2.3: There exists an "optimal rainy season length" for relative changes in ecosystem productivity across large MAP ranges (the white area between the red and blue space in Figure 5e). For the same MAP, any deviation of T_w from the "optimal rainy season length" would reduce GPP. This "optimal rainy season length" follows an increasing trend with MAP until 1400 mm/year.

Figure 6c explains the hydrological mechanism for the negative GPP sensitivity in Pattern 2.1. In the situation with low MAP and infrequent rainfall events, decreasing rainfall frequency and expanding rainy season length (i.e. $T_w\uparrow$, $\lambda\downarrow$) would lead to longer intervals between rainfall events and possibly longer excursions below S_w, which would disrupt continuous plant growth and have detrimental effects on ecosystem productivity. It is worth noting that long rainy season in dryland (Figure 5e) is usually accompanied with low rainfall frequency (Figure 5g). The southern African drylands (south of 15℃S) typically fall in this category, and these regions thus have negative GPP sensitivity (Figure 4c and 4d), accompanied by a small biome conversion from woodlands to grasslands (Figure 3b).

Figure 6d explains the hydrological mechanisms for the positive GPP sensitivity in Pattern 2.2. When rainfall is ample enough to maintain little or no water stress during rainy season, increasing the interval of rainfall events may introduce little additional water stress but can significantly extend the growing season. This situation mostly happens in woodlands, where limited water stress exists during rainy season, and dry season length is the major constraint for plant growth. Thus the increase of rainy season length extends the temporal niche for plant growth, and leads to a significant woodland expansion to grasslands as well as an expansion of tropical evergreen forests to woodlands (Figure 3b).

The little GPP sensitivity in tropical evergreen forest regions is mostly attributed to the long rainy season length in this ecosystem. Thus further increasing T_w may reach to its saturation (365 days) and has little impact to ecosystem productivity. This also explains why the magnitude of GPP sensitivity is much smaller at high MAP range than at the intermediate MAP range.

The finding of "optimal rainy season length" across different rainfall regimes (Figure 5e) is consistent with our previous empirical finding about the similar pattern of "optimal rainy season length" for tree fractional cover in Africa derived based on a satellite remote sensing product (Guan et al., 2014). The existence of "optimal rainy season length" fully demonstrates the importance to explicitly consider the non-linear impacts of rainy season length on ecosystem productivity under climate change, which has been largely overlooked before.

3.3 Ecosystem sensitivity to rainfall seasonality and intensity ($S_{Tw-\alpha}$)

Results of Experiment $S_{Tw-\alpha}$ have many similarities with those of $S_{Tw-\lambda}$, including the similar changes in biome distributions (Figure 3), soil moisture and GPP patterns (Figure 4e and 4f). We further find that the GPP sensitivity space with MAP and rainy season length for $S_{Tw-\alpha}$ (Figure 5i) is also similar with that for $S_{Tw-\lambda}$ (Figure 5e). One new finding is that rainfall intensity has little impact on GPP, as the contour lines in Figure 5k are mostly parallel with y-axis (i.e. rainfall intensity).

Figure 6e and 6f explain the governing hydrological mechanisms for the patterns of $S_{Tw-\alpha}$, which also have many similarities with $S_{Tw-\lambda}$. For the negative case (Figure 6e), decreasing rainfall intensity and increasing rainy season length in the very low MAP regime may lead to more downcrossings of S_w and interrupt continuous plant growth. The positive case (Figure 6e) is similar as that in Figure 6d, i.e. the repartitioning of excessive wet-season rainfall to the dry season for an extended growing period would significantly benefit plant growth and possible increase tree fraction cover.

4. Discussion

In this paper we provide a new modeling approach to systematically interpret the ecological impacts from changes in intra-seasonal rainfall characteristics (i.e. rainfall frequency, rainfall intensity and rainy season length) across biomes and climate gradients in the African continent.

4.1 Limitation of the methodology

Though our modeling framework is able to characterize the diverse ecosystem responses to the shifts in different rainfall characteristics, it nevertheless has its limitations. The current rainfall model only deals with the case of single rainy season per year, and approximates the case of double rainy seasons per year to be the single rainy season case. This assumption may induce unrealistic synthetic rainfall patterns in the equatorial dryland regions, in particular the Horn of Africa. Thus the simulated sensitivity of these regions may be less reliable. We also assume that rainfall frequency and intensity are homogenous throughout wet seasons (or dry seasons), but in reality they have seasonal variations. We only consider rainy season length for rainfall seasonality, and neglect the possible temporal phase change; in reality, rainfall seasonality change usually has length and phase shifts in concert. These rainfall-model-related limitations can be possibly overcame by simulating smaller intervals of rainfall processes (e.g. each month has their own α and λ) rather than simulating the whole wet or dry season using one fixed set of α and λ. However, we need to point out that our weather generator provides a good performance (Figure S1 and S2) with almost a constant bias (i.e. interceptions in Figure S2); besides, the time-varying phenology schemes in SEIB, as well as the current focus of the relative change of GPP (through normalizing with the baseline simulation result), have further reduced the possible errors of the absolute difference of simulated GPP. Furthermore, our approach has been an improvement by explicitly including the rainy season length to the original Marked Poisson Process-based rainfall model (Rodríguez-Iturbe et al., 1984). We thus believe that our study carries its novelty, and our results are robust and reliable at the continental scale.

In addition, only using one ecosystem model here means that the simulated ecosystem sensitivity can be model-specific. Though magnitudes or thresholds for the corresponding patterns may vary depending on different models, we argue that the qualitative results for the GPP sensitivity patterns (e.g. Figure 4 and Figure 5) should hold as the necessary ecohydrological processes have been incorporated in SEIB-DGVM. We also recognize that to exclude fire impacts in the current simulation may bring some limitation for this study, as evidence shows that many savanna regions can be bistable due to fire effects (Staver et al 2011; Hirota et al 2011; Higgins and Scheiter 2012; also see for a possible rebuttal in Hanan et al, 2013). Changes in rainfall regimes not only have direct effects on vegetation productivity, but can also indirectly affect ecosystems through its interactions with fire, with rapid biome shifts being a possible consequence. These feedbacks can be important in situations when the changes in growing season length are related to fuel loads, fuel moisture dynamics and hence fire intensity (Lehmann et al., 2011). Quantifying these fire-rainfall feedbacks will be the important future direction to pursue.

4.2 Clarifying the impacts of rainfall frequency and intensity on ecosystem productivity

In this modeling study, we provide a plausible answer to possibly resolve the previous debate about whether increasing rainfall intensity (or equivalently decreasing rainfall frequency, i.e. $\lambda\downarrow$, $\alpha\uparrow$) has positive or negative impacts on above-ground primary productivity under a fixed annual rainfall total. We identify that negative GPP sensitivity with increased rainfall frequency is possible at very low MAP range (~ 400 mm/year) with relatively low rainfall frequency (<0.35 event/day) (Figure 5a), due to the increased downcrossings of soil moisture wilting point, which restricts plant growth (Figure 6a). This derived MAP threshold (~400 mm/year) is consistent with our meta-analysis based on the previous field studies (Table 1), which shows a threshold of MAP at 340 mm/year separates positive and negative impacts of more intense rainfall on aboveground net primary production (ANPP). Our findings are also consistent with another study about increased tree encroachments with increased

rainfall intensity in low rainfall regime (<544mm/year, Kulmatiski and Beard, 2013), which essentially follows the same mechanism as identified in Figure 6a.

In addition, we thoroughly investigated the ecosystem responses across a wide range of annual rainfall in Africa. We find that beyond the very low rainfall range (below 400 mm/year), most grasslands and woodlands would benefit from increasing rainfall frequency, which also corroborate the previous large-scale findings about the positive effects of increased rainfall frequency (and decreased rainfall intensity) for tree fractions across the African continent (Good and Caylor, 2011). The only exception happens at the very wet end of MAP (~1800mm/year) where cloud-induced radiation-limitation may suppress ecosystem productivity with increased rainfall frequency. We also find that changes in rainfall frequency and intensity mostly affect grassland-dominated savannas (changes of GPP up to 20%), and the corresponding effects are much smaller in woodlands and have little impact on woodland distribution. Though this work is only based on a single model, it provides a primary assessment for understanding of interactive changes between λ and α in ecosystem functioning, and expands the analysis to a wide range of annual rainfall conditions compared with previous studies (e.g. Porporato et al., 2004).

4.3 Ecological importance of rainy season length

The results involving rainy season length (i.e. $S_{Tw-\lambda}$ and $S_{Tw-\alpha}$) provide evidence for the ecological importance of rainfall seasonality. The magnitudes of changes in soil moisture, GPP and biome distribution in $S_{Tw-\lambda}$ and $S_{Tw-\alpha}$ are much larger than those of $S_{\lambda-\alpha,}$ with almost one order of magnitude difference. These disproportional impacts of T_w indicate that slight changes in rainy season length could modify biome distribution and ecosystem function more dramatically compared with the same percentage changes in rainfall frequency and intensity. We also notice that $S_{Tw-\lambda}$ and $S_{Tw-\alpha}$ have similar results. This is because that both λ and α describe rainfall characteristics within wet season, while T_w describes rainfall characteristics of both dry season and wet season. It is noted that our treatment of changing rainy season length while assuming the homogeneity of rainfall statistics (i.e. frequency and intensity) within

598 the rainy season may slightly overestimate the importance of rainy season length.

599 Given the importance of rainy season length, its ecological impacts under climate
600 change are largely understudied, though substantial shifts in rainfall seasonality have
601 been projected in both Sahel and South Africa (Biasutti and Sobel, 2009; Shongwe et
602 al., 2009; Seth et al., 2013). Here we only address the rainfall seasonality in terms of
603 its length, and future changes in rainfall seasonality may modify their phase and
604 magnitude in concert. The climate community has focused on the increase of extreme
605 rainfall events (Field et al., 2012), which could be captured by the changes in λ or α
606 towards heavier tails in their distribution. However, explicit and systematic
607 assessments and projection on rainfall seasonality changes (including both phase and
608 magnitude) are still limited even in the latest Intergovernmental Panel on Climate
609 Change (IPCC) synthesis reports (Field et al., 2012; Stocker et al., 2013). More
610 detailed studies related to these changes and their ecological implications are required
611 for future hydroclimate-ecosystem research.

612

613 **4.4 Not all rainfall regimes are ecologically equivalent**

614 As Figure 1 gives a convincing example that the same total annual rainfall may arrive
615 in a very different way, our results further demonstrate that ecosystems respond
616 differently to the changes in these intra-seasonal rainfall variability. For example, with
617 similar MAP, drylands in West Africa and Southwest Africa show reversed responses
618 to the same changes in intra-seasonal rainfall variability. As shown in the experiments
619 of $S_{Tw-\lambda}$ and $S_{Tw-\alpha}$, increasing T_w while decreasing λ or α generates slightly positive
620 soil moisture and GPP sensitivity in West Africa (Figure 4c and 4d), but would cause
621 relatively large GPP decrease in Southwest Africa. The prior hydroclimate conditions
622 of these two regions can explain these differences: West Africa has much shorter rainy
623 season with more intense rainfall events; in contrast, Southwest Africa has a long
624 rainy season but many small and sporadic rainfall events. As a result, under a fixed
625 annual rainfall total, slightly increasing rainy season and meanwhile decreasing
626 rainfall intensity would benefit plant growth in West Africa, but the same change
627 would lengthen dry spells in Southwest Africa and bring negative effects to the

ecosystem productivity. We further deduce that the rainfall use efficiency (RUE, defined as the ratio of plant net primary production to total rainfall amount) in these two drylands could be different: West Africa may have lower RUE, and the intense rainfall could lead to more infiltration-excess runoff, and thus less water would be used by plants; while Southwest Africa can have higher RUE, because its sporadic and feeble rainfall events would favor grass to fully take the advantage of the ephemerally existed water resources. This conclusion is partly supported by Martiny et al. (2007) based on satellite remote sensing. We further hypothesize that landscape geomorphology in these two drylands may be different and therefore reflect distinctive rainfall characteristics. More bare soil may exist in West Africa grasslands due to intense-rainfall-induced erosion, while Southwest Africa may have more grass fraction and less bare soil fraction. Testing these interesting hypotheses is beyond the scope of this paper, but is worthy the further exploration.

Acknowledgements:

K. Guan and E. F. Wood acknowledge the financial supports from the NASA NESSF fellowship. S.P. Good and K. K. Caylor acknowledge the financial supports from the National Science Foundation through the Grant EAR-0847368. The authors thank Ignacio Rodr ǵuez-Iturbe for his valuable inputs and discussion.

References:

Anderegg, L. D. L.; Anderegg, W. R. L. & Berry, J. A. (2013), 'Not all droughts are created equal: translating meteorological drought into woody plant mortality', *Tree Physiology* **33**, 701-712.

Bates, J.; Svejcar, T.; Miller, R. & Angell, R. (2006), 'The effects of precipitation timing on sagebrush steppe vegetation', *Journal of Arid Environments* **64**, 670-697.

Biasutti, M. & Sobel, A. H. (2009), 'Delayed Sahel rainfall and global seasonal cycle in a warmer climate', *Geophysical Research Letters* **36, L23707**.

Bond, W. J.; Woodward, F. I. & Midgley, G. F. (2005), 'The Global Distribution of Ecosystems in a World without Fire', *New Phytologist* **165(2)**, 525-537.

Easterling, D. R.; Meehl, G. A.; Parmesan, C.; Changnon, S. A.; Karl, T. R. & Mearns, L. O. (2000), 'Climate Extremes: Observations, Modeling, and Impacts', *Science* **289**, 2068-2074.

Fang, J.; Piao, S.; Zhou, L.; He, J.; Wei, F.; Myneni, R. B.; Tucker, C. J. & Tan, K. (2005), 'Precipitation patterns alter growth of temperate vegetation', *Geophysical Research Letters* **32, L21411**.

Fay, P. A.; Carlisle, J. D.; Knapp, A. K.; Blair, J. M. & Collins, S. L. (2003), 'Productivity responses to altered rainfall patterns in a C4-dominated grassland', *Oecologia* **137**, 245-251.

Feng, X.; Porporato, A. & Rodriguez-Iturbe, I. (2013), 'Changes in rainfall seasonality in the tropics', *Nature Climate Change*.

Field, C.; Barros, V.; Stocker, T.; Qin, D.; Dokken, D.; Ebi, K.; Mastrandrea, M.; Mach, K.; Plattner, G.-K.; Allen, S.; Tignor, M. & Midgley, P., ed. (2012), *IPCC, 2012: Managing the Risks of Extreme Events and Disasters to Advance Climate Change Adaptation. A Special Report of Working Groups I and II of the Intergovernmental Panel on Climate Change*, Cambridge University Press, Cambridge, UK, and New York, NY, USA.

Franz, T. E.; Caylor, K. K.; Nordbotten, J. M.; Rodr ǵuez-Iturbe, I. & Celia, M. A. (2010), 'An ecohydrological approach to predicting regional woody species distribution patterns in dryland ecosystems', *Advances in Water Resources* **33(2)**, 215-230.

Gerten, D.; Luo, Y.; Maire, G. L.; Parton, W. J.; Keougn, C.; Weng, E.; Beier, C.; Ciais, P.; Cramer, W.; Dukes, J. S.; Hanson, P. J.; Knapp, A. A. K.; Linder, S.; Nepstad, D.; Rustad, L. & Sowerby, A. (2008), 'Modelled effects of precipitation on ecosystem carbon and water dynamics in different climatic zones', *Global Change Biology* **14**,

694 2365-2379.
695
696 Good, S. P. & Caylor, K. K. (2011), 'Climatological determinants of woody cover in
697 Africa', *Proceedings of the National Academy of Sciences of United States of America*
698 **108(12)**, 4902-4907.
699
700 Graham, E. A.; Mulkey, S. S.; Kitajima, K.; Phillips, N. G. & Wright, S. J. (2003),
701 'Cloud cover limits net CO2 uptake and growth of a rainforest tree during tropical
702 rainy seasons', *Proceedings of the National Academy of Sciences of the United States*
703 *of America* **100(2)**, 572-576.
704
705 Guan, K.; Wood, E. F. & Caylor, K. K. (2012), 'Multi-sensor derivation of regional
706 vegetation fractional cover in Africa', *Remote Sensing of Environment* **124**, 653-665.
707
708 Guan, K.; Wood, E. F.; Medvigy, D.; Pan, M.; Caylor, K. K.; Sheffield, J.; Kimball, J.;
709 Xu, X. & Jones, M. O. (2014), 'Terrestrial hydrological controls on vegetation
710 phenology of African savannas and woodlands', *Journal of Geophysical Research*.
711
712 Hanan, N. P.; Tredennick, A. T.; Prihodko, L.; Bucini, G. & Dohn, J. (2013), 'Analysis
713 of stable states in global savannas: is the CART pulling the horse?', *Global Ecology and*
714 *Biogeography* **23(3)**, 259-263.
715
716 Harper, C. W.; Blair, J. M.; Fay, P. A.; Knapp, A. K. & Carlisle, J. D. (2005), 'Increased
717 rainfall variability and reduced rainfall amount decreases soil CO2 flux in a grassland
718 ecosystem', *Global Change Biology* **11**, 322-334.
719
720 Heisler-White, J. L.; Blair, J. M.; Kelly, E. F.; Harmoney, K. & Knapp, A. K. (2009),
721 'Contingent productivity responses to more extreme rainfall regimes across a grassland
722 biome', *Global Change Biology* **15(12)**, 2894-2904.
723
724 Hđy, C.; Bremond, L.; Alleaume, S.; Smith, B.; Sykes, M. T. & Guiot, J. (2006),
725 'Sensitivity of African biomes to changes in the precipitation regime', *Global Ecology*
726 *and Biogeography* **15**, 258-270.
727
728 Hirota, M.; Holmgren, M.; Nes, E. H. V. & Scheffer, M. (2011), 'Global Resilience of
729 Tropical Forest and Savanna to Critical Transitions', *Science* **334**, 232-235.
730
731 Higgins, S. I. & Scheiter, S. (2012), 'Atmospheric CO2 forces abrupt vegetation shifts
732 locally, but not globally', *Nature* **488**, 209-212.
733
734 Holmgren, M.; Hirota, M.; van Nes, E. H. & Scheffer, M. (2013), 'Effects of
735 interannual climate variability on tropical tree cover', *Nature Climate Change*.
736
737 Huffman, G. J.; Bolvin, D. T.; Nelkin, E. J.; Wolff, D. B.; Adler, R. F.; Bowman, K. P.

& Stocker, E. F. (2007), 'The TRMM Multisatellite Precipitation Analysis (TMPA): Quasi-Global, Multiyear, Combined-Sensor Precipitation Estimates at Fine Scales', *Journal of Hydrometeorology* **8**, 38-55.

Knapp, A. K.; Fay, P. A.; Blair, J. M.; Collins, S. L.; Smith, M. D.; Carlisle, J. D.; Harper, C. W.; Danner, B. T.; Lett, M. S. & McCarron, J. K. (2002), 'Rainfall Variability, Carbon Cycling, and Plant Species Diversity in a Mesic Grassland', *Science* **298**, 2202-2205.

Kulmatiski, A. & Beard, K. H. (2013), 'Woody plant encroachment facilitated by increased precipitation intensity', *Nature Climate Change*.

Lehmann, C. E. R.; Archibald, S. A.; Hoffmann, W. A. & Bond, W. J. (2011), 'Deciphering the distribution of the savanna biome', *New Phytologist* **191**, 197-209.

Markham, C. (1970), 'Seasonality of precipitation in the United States', *Annals of the Association of American Geographers* **60(3)**, 593-597.

Martiny, N.; Camberlin, P.; Richard, Y. & Philippon, N. (2006), 'Compared regimes of NDVI and rainfall in semi-arid regions of Africa', *International Journal of Remote Sensing* **27(23)**, 5201-5223.

Miranda, J.; Armas, C.; Padilla, F. & Pugnaire, F. (2011), 'Climatic change and rainfall patterns: Effects on semi-arid plant communities of the Iberian Southeast', *Journal of Arid Environments* **75**, 1302-1309.

Nemani, R. R.; Keeling, C. D.; Hashimoto, H.; Jolly, W. M.; Piper, S. C.; Tucker, C. J.; Myneni, R. B. & Running, S. W. (2003), 'Climate-Driven Increases in Global Terrestrial Net Primary Production from 1982 to 1999', *Science* **300**, 1560-1563.

O'Gorman, P. A. & Schneider, T. (2009), 'The physical basis for increases in precipitation extremes in simulations of 21st-century climate change', *Proceedings of the National Academy of Sciences of the United States of America* **106(35)**, 14773-14777.

Porporato, A.; Daly, E. & Rodr ́guez-Iturbe, I. (2004), 'Soil Water Balance and Ecosystem Response to Climate Change', *American Naturalist* **164(5)**, 625-632.

Porporato, A.; Laio, F.; Ridolfi, L. & Rodr ́guez-Iturbe, I. (2001), 'Plants in water-controlled ecosystems: active role in hydrologic processes and response to water stress - III. Vegetation water stress', *Advances in Water Resources* **24(7)**, 725-744.

Robertson, T. R.; Bell, C. W.; Zak, J. C. & Tissue, D. T. (2009), 'Precipitation timing and magnitude differentially affect aboveground annual net primary productivity in

three perennial species in a Chihuahuan Desert grassland', *New Phytologist* **181**, 230-242.

Rodr ́guez-Iturbe, I.; Gupta, V. K. & Waymire, E. (1984), 'Scale Considerations in the Modeling of Temporal Rainfall', *Water Resource Research* **20(11)**, 1611-1619.

Rodr ́guez-Iturbe, I. & Porporato, A. (2004), *Ecohydrology of Water-Controlled Ecosystems: Soil Moisture And Plant Dynamics*, Cambridge University Press.

Rodr ́guez-Iturbe, I.; Porporato, A.; Ridolfi, L.; Isham, V. & Cox, D. R. (1999), 'Probabilistic Modelling of Water Balance at a Point: The Role of Climate, Soil and Vegetation', *Proceedings: Mathematical, Physical and Engineering Sciences* **455**, 3789-3805.

Ross, I.; Misson, L.; Rambal, S.; Arneth, A.; Scott, R. L.; Carrara, A.; Cescatti, A. & Genesio, L. (2012), 'How do variations in the temporal distribution of rainfall events affect ecosystem fuxes in seasonally water-limited Northern Hemisphere shrublands and forests?', *Biogeosciences* **9**, 1007-1024.

Saha, S.; Moorthi, S.; Pan, H.-L.; Wu, X.; Wang, J.; Nadiga, S.; Tripp, P.; Kistler, R.; Woollen, J.; Behringer, D.; Liu, H.; Stokes, D.; Grumbine, R.; Gayno, G.; Wang, J.; Hou, Y.-T.; Chuang, H.-Y.; Juang, H.-M. H.; Sela, J.; Iredell, M.; Treadon, R.; Kleist, D.; Delst, P. V.; Keyser, D.; Derber, J.; Ek, M.; Meng, J.; Wei, H.; Yang, R.; Lord, S.; Dool, H. V. D.; Kumar, A.; Wang, W.; Long, C.; Chelliah, M.; Feng, Y.; Huang, B.; Schemm, J.-K.; Ebisuzaki, W.; Lin, R.; Xie, P.; Chen, M.; Zhou, S.; Higgins, W.; Zou, C.-Z.; Liu, Q.; Chen, Y.; Han, Y.; Cucurull, L.; Reynolds, R. W.; Rutledge, G. & Goldberg, M. (2010), 'The NCEP Climate Forecast System Reanalysis', *Bulletin of the American Meteorological Society* **91**, 1015-1057.

Sato, H. (2009), 'Simulation of the vegetation structure and function in a Malaysian tropical rain forest using the individual-based dynamic vegetation model SEIB-DGVM', *Forest Ecology and Management* **257**, 2277-2286.

Sato, H. & Ise, T. (2012), 'Effect of plant dynamic processes on African vegetation responses to climate change: analysis using the spatially explicit individual-based dynamic global vegetation model (SEIB-DGVM)', *Journal of Geophysical Research* **117, G03017**.

Sato, H.; Itoh, A. & Kohyama, T. (2007), 'SEIB-DGVM: A new Dynamic Global Vegetation Model using a spatially explicit individual-based approach', *Ecological Modelling* **200(3-4)**, 279-307.

Sato, H.; Kobayashi, H. & Delbart, N. (2010), 'Simulation study of the vegetation structure and function in eastern Siberian larch forests using the individual-based

vegetation model SEIB-DGVM', *Forest Ecology and Management* **259**, 301-311.

Scanlon, T. M.; Caylor, K. K.; Manfreda, S.; Levin, S. A. & Rodriguez-Iturbe, I. (2005), 'Dynamic response of grass cover to rainfall variability: implications for the function and persistence of savanna ecosystems', *Advances in Water Resources* **28**, 291-302.

Shugart, H. H. (1998), 'Terrestrial ecosystems in changing environments', Cambridge University Press, United Kingdom.

van Schaik, C. P.; Terborgh, J. W. & Wright, S. J. (1993), 'The Phenology of Tropical Forests: Adaptive Significance and Consequences for PrimaryConsumers', *Annual Review of Ecology and Systematics* **24**, 353-377.

Scholes, R. J. & Archer, S. R. (1997), 'Tree-Grass Interactions in Savannas', *Annual Review of Ecology and Systematics* **28**, 517-544.

Seth, A.; Rauscher, S. A.; Biasutti, M.; Giannini, A.; Camargo, S. J. & Rojas, M. (2013), 'CMIP5 Projected Changes in the Annual Cycle of Precipitation in Monsoon Regions', *Journal of Climate* **26**, 7328-7351.

Sheffield, J.; Goteti, G. & Wood, E. F. (2006), 'Development of a 50-Year High-Resolution Global Dataset of Meteorological Forcings for Land Surface Modeling', *Journal of Climate* **19**, 3088-3111.

Shongwe, M. E.; van Oldenborgh, G. J.; van den Hurk, B. J. J. M.; de Boer, B.; Coelho, C. A. S. & van Aalst, M. K. (2009), 'Projected Changes in Mean and Extreme Precipitation in Africa under Global Warming. Part I: Southern Africa', *Journal of Climate* **22**, 3819-3837.

Staver, A. C.; Archibald, S. & Levin, S. A. (2011), 'The Global Extent and Determinants of Savanna and Forest as Alternative Biome States', *Science* **334**, 230-232.

Stocker, T. F.; Qin, D.; Plattner, G.-K.; Tignor, M.; Allen, S. K.; Boschung, J.; Nauels, A.; Xia, Y.; Bex, V. & Midgley, P. M., ed. (2013), *IPCC, 2013: Climate Change 2013: The Physical Science Basis. Contribution of Working Group I to the Fifth Assessment Report of the Intergovernmental Panel on Climate Change*, Cambridge University Press, Cambridge, United Kingdom and New York, NY, USA..

Svejcar, T.; Bates, J.; Angell, R. & Miller, R. (2003), 'The influence of precipitation timing on the sagebrush steppe ecosystem. In: Guy, McPherson, Jake, Weltzin (Eds.), Changing Precipitation Regimes &Terrestrial Ecosystems. University of Arizona Press, Tucson, AZ 237pp.', .

Thomey, M. L.; Collins, S. L.; Vargas, R.; Johnson, J. E.; Brown, R. F.; Natvig, D. O. & Friggens, M. T. (2011), 'Effect of precipitation variability on net primary production and soil respiration in a Chihuahuan Desert grassland', *Global Change Biology* **17**, 1505-1515.

Trenberth, K. E.; Dai, A.; Rasmussen, R. M. & Parsons, D. B. (2003), 'The Changing Character of Precipitation', *Bulletin of American Meterological Society* **84**, 1205-1217.

Vincens, A.; Garcin, Y. & Buchet, G. (2007), 'Influence of rainfall seasonality on African lowland vegetation during the Late Quaternary: pollen evidence from Lake Masoko, Tanzania', *Journal of Biogeography* **34**, 1274-1288.

Weltzin, J. F.; Loik, M. E.; Schwinning, S.; Williams, D. G.; Fay, P. A.; Haddad, B. M.; Harte, J.; Huxman, T. E.; Knapp, A. K.; Lin, G.; Pockman, W. T.; Shaw, M. R.; Small, E. E.; Smith, M. D.; Smith, S. D.; Tissue, D. T. & Zak, J. C. (2003), 'Assessing the Response of Terrestrial Ecosystems to Potential Changes in Precipitation', *BioScience* **53(10)**, 941-952.

Williams, C. A. & Albertson, J. D. (2006), 'Dynamical effects of the statistical structure of annual rainfall on dryland vegetation', *Global Change Biology* **12**, 777-792.

Zhang, X.; Friedl, M. A.; Schaaf, C. B.; Strahler, A. H. & Liu, Z. (2005), 'Monitoring the response of vegetation phenology to precipitation in Africa by coupling MODIS and TRMM instruments', *Journal of Geophysical Research* **110, D12103**.

Zhang, Y.; Moran, M. S.; Nearing, M. A.; Campos, G. E. P.; Huete, A. R.; Buda, A. R.; Bosch, D. D.; Gunter, S. A.; Kitchen, S. G.; McNab, W. H.; Morgan, J. A.; McClaran, M. P.; Montoya, D. S.; Peters, D. P. & Starks, P. J. (2013), 'Extreme precipitation patterns and reductions of terrestrial ecosystem production across biomes', *Journal of Geophysical Research: Biogeosciences* **118**, 148-157.

Table 1. Summary of previous representative studies on assessing the impacts of rainfall characteristics (i.e. rainfall frequency, intensity and seasonality) on the structure and function of terrestrial ecosystem.

Focus: frequency (freq); intensity (int); seasonality (sea); variation (CV).

Methods: Field Experiments (Field); Remote Sensing (RS); Flux Tower (Flux).

Major Conclusion: increasing rainfall intensity (or decreasing frequency) has positive impacts (int+); increasing intensity (or decreasing frequency)has negative impacts (int-); increasing rainfall CV has positive impacts (CV+); increasing rainfall CV has negative impacts (CV-).

Focus	Methods	Spatial Scale	Time scale	MAP (mm/year)	Ecosystem type	Major Conclusion	Reference
freq; int	RS	Africa continent	intra-annual climatology	[0,3000]	Africa all	(int-) woody cover	Good and Caylor, 2011
freq; int	RS	US		[163,1227]	US	(int-) ANPP greatest in arid grassland (16%)and Mediterranean forest (20%) and less for mesic grassland and temperate forest (3%)	Zhang et al., 2013
freq; int	RS	Pan-tropics (35 °N to 15 °S)	inter-annual	[0,3000]	Tropical ecosystems	(CV+) wood cover in dry tropics; (CV-) wood cover in wet tropics	Holmgren et al., 2013
freq; int	RS	Northern China	intra-annual	[100,850]	temperate grassland and forests	(int-) NDVI for temprate grassland and broadleaf forests, not for coniferous forest	Fang et al., 2005
freq; int	Flux	Northern Hemisphere	intra-annual	[393±155,906±243]	shrubland and forest	(int-) GPP, RE and NEP	Ross et al., 2012
seas	RS	Africa continent	climatology	[0,3000]	Africa all	rainy season onset and offset controls vegetation growing season	Zhang et al., 2005
freq; int	Field	plot (Kansas, USA)	intra-annual	615	grassland	(int-) ANPP	Knapp et al., 2002

(fix MAP)							
freq; int (fix MAP)	Field	plot (Kansas, USA)	intra-annual	835	grassland	(int-) ANPP	Fay et al., 2003
increase seasonal rainfall	Field	plot(Taxes, USA)	intra-annual	365	grassland	(int-) ANPP	Robertson et al., 2009
freq; int	Field	plot (Kansas, USA)	intra-annual	[320,830]	grassland	(int-)ANPP for MAP=830mm/yr; (int+)ANPP for MAP=320mm/yr	Heisler-White et al., 2009
freq; int	Field	plot(New Mexico, USA)	intra-annual	250	grassland	(int+) ANPP	Thomey et al., 2011
freq; int (fix MAP)	Field	Plot(Kansas, USA)	intra-annual	834	grassland	(int-) soil CO2 flux	Harper et al., 2005
freq; int (fix MAP)	Field	plot(Kruger National Park, South Africa)	intra-annual	544	sub-tropical savanna	(int+) wood growth; (int-) grass growth	Kulmatiski and Beard, 2013
sea (fix MAP)	Field	plot(Oregon, USA)	intra-annual	[140,530]	grassland	impact biomass and bare soil fraction	Bates et al., 2006; Svejcar et al., 2003
sea	Field						
freq; int; MAP	Field	plot(South Africa)	intra-annual	[538,798]	grassland	(int-) ANPP	Swemmer et al., 2007
MAP; sea	Field	plot(Spain)	intra-/inter-annual	242	grassland	Mediterranean dryland ecosystem has more resilience for intra- and inter-annual changes in rainfall	Miranda et al., 2008

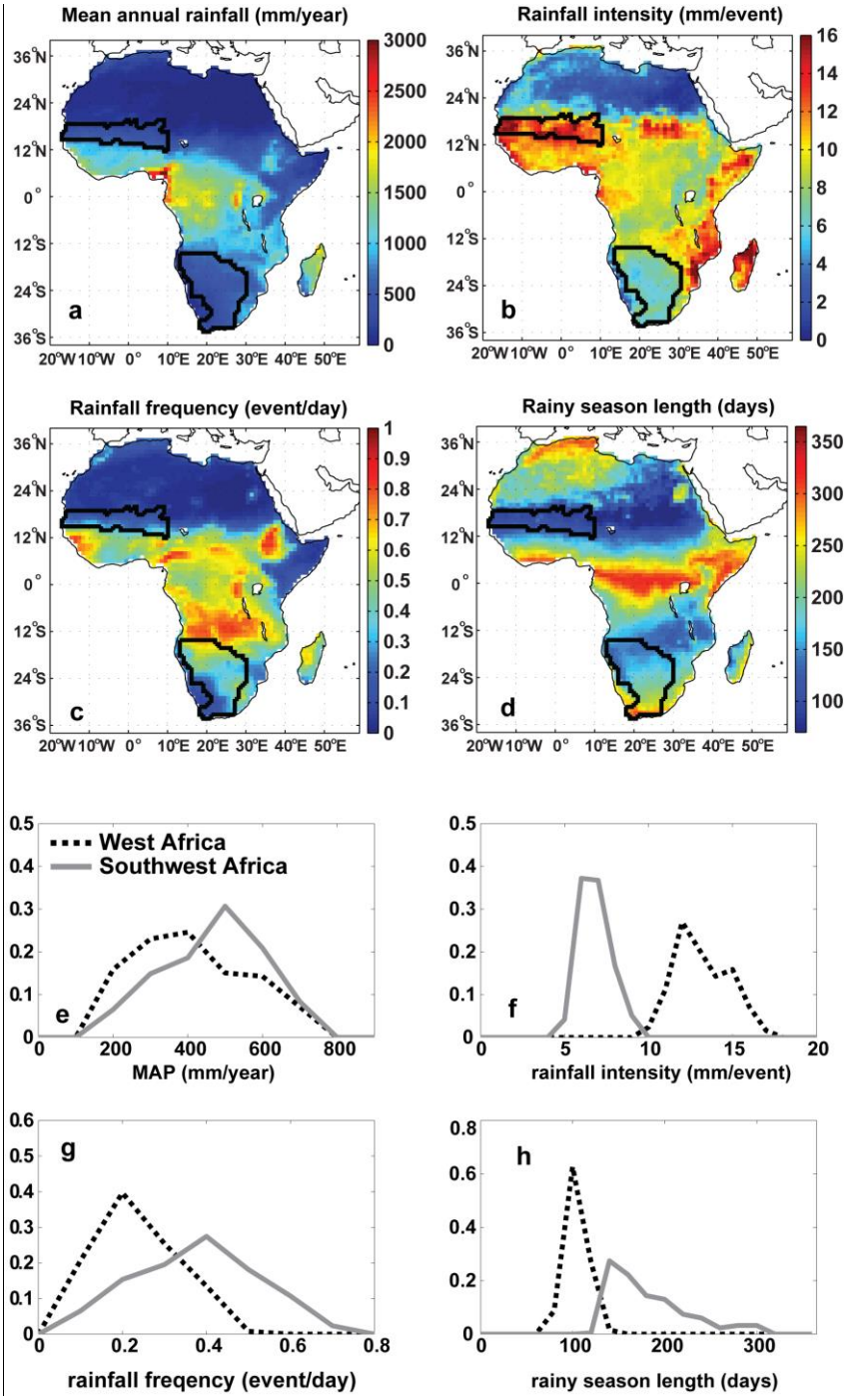

Figure 1. a-b: Spatial pattern of the rainfall characteristics in Africa: a-MAP; b-rainfall intensity; c-rainfall frequency; d-rainy season length. The black-line identified areas refer to two savanna regions in West and Southwest Africa. e-f: Normalized histograms of the rainfall characteristics in two savanna regions of West and Southwest Africa. e-MAP (bin width for the x-axis: 100 mm/year); f-rainfall intensity (bin width for the x-axis: 1 mm/event); g-rainfall frequency (bin width for the x-axis: 0.1 event/day); h-rainy season length (bin width for the x-axis: 20 days).

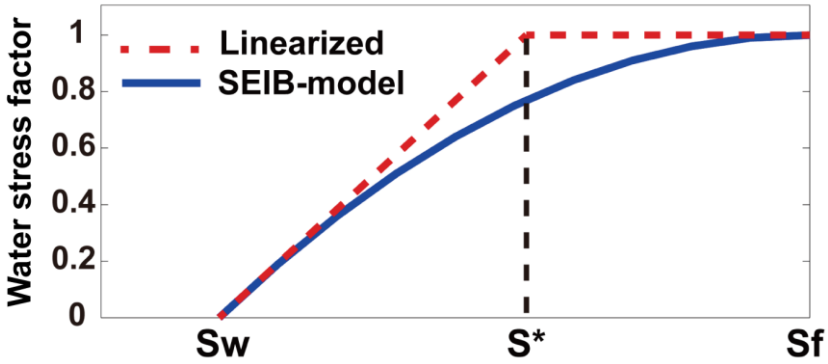

Figure 2. Schematic diagram of water stress factor ranging from 0 (most stressful) to 1 (no stress), which acts to reduce transpiration and carbon assimilation. The red dotted line is based on Porporato et al. (2001) with a reversed sign, and SEIB-DGVM has a nonlinear implementation (blue solid line, Sato and Ise, 2012).

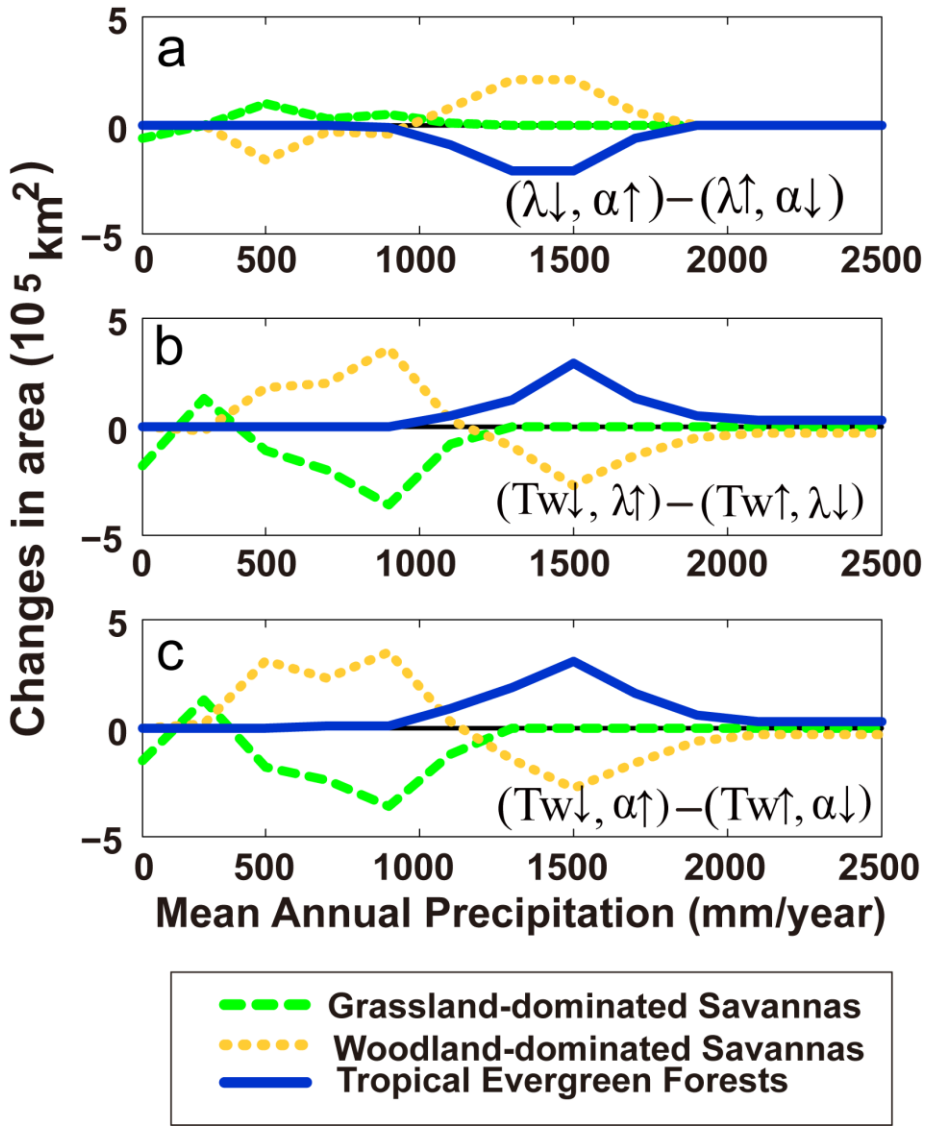

Figure 3. Differences in simulated dominated biomes in the three experiments (i.e. $S_{\lambda-\alpha}$, $S_{Tw-\lambda}$, $S_{Tw-\alpha}$).

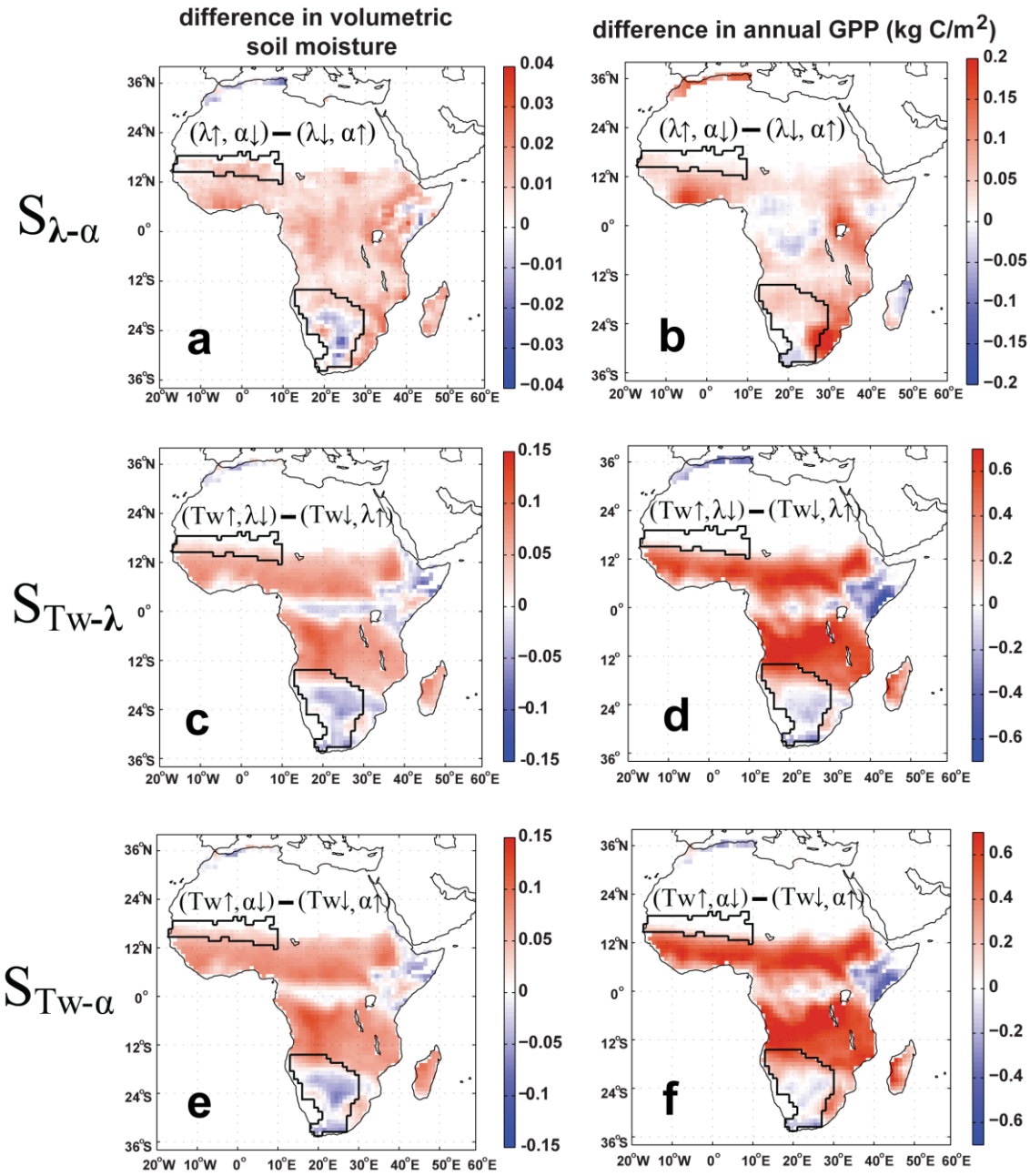

Figure 4. Simulated changes in annual mean soil moisture (0-500mm, first column) and annual mean GPP (second column) for different experiments. Please note that the scales of $S_{\lambda-\alpha}$ is much smaller than those of $S_{Tw-\lambda}$ and $S_{Tw-\alpha}$. The two areas with black boundaries in each panel are West African grassland and Southwest African grassland associated with Figure 1. The spatial patterns shown here are smoothed by 3*3 smoothing window from the raw data.

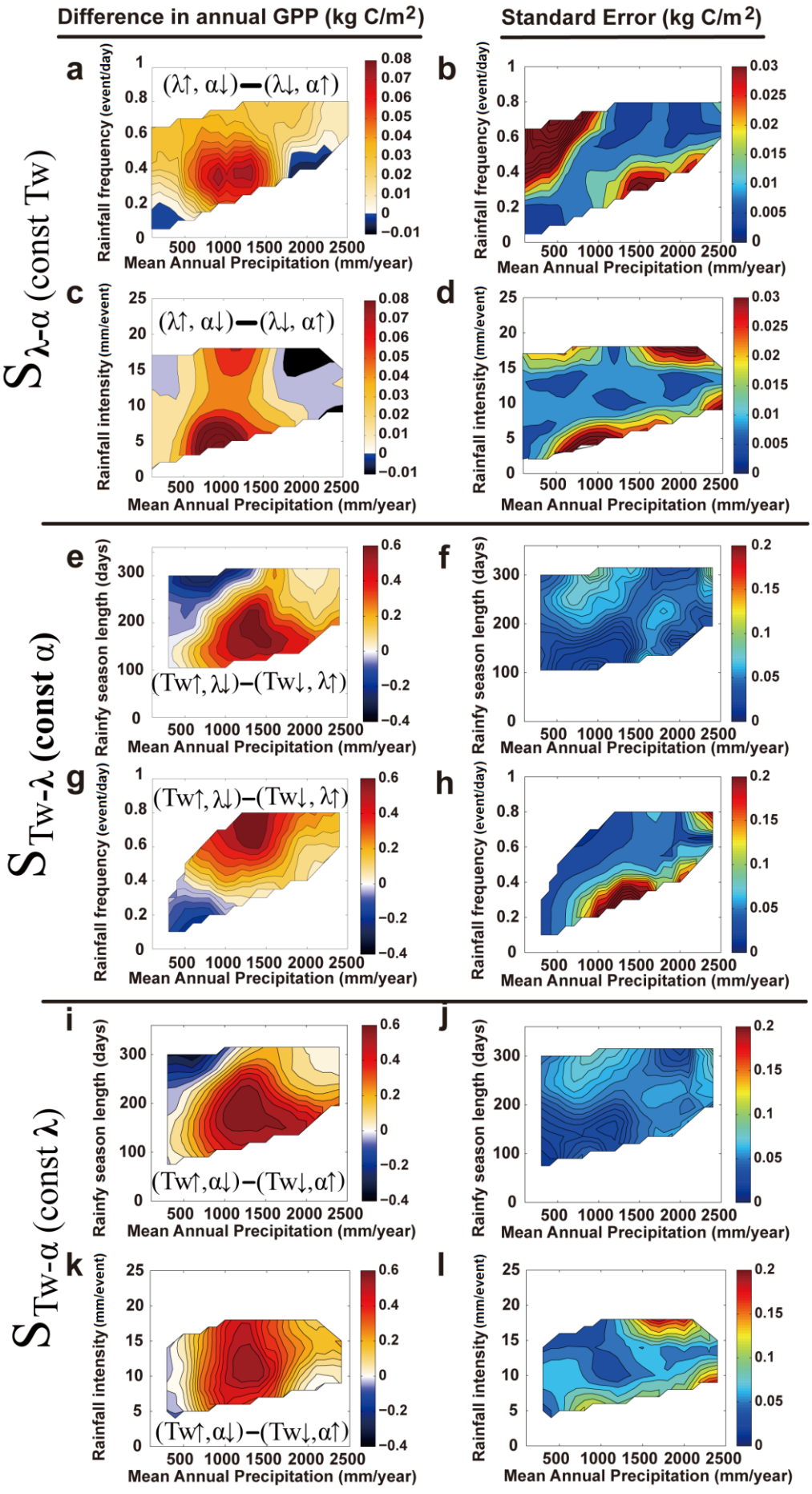
Difference in annual GPP (kg C/m2)
Standard Error (kg C/m2)
$S_{\lambda\text{-}\alpha}$ (const Tw)
$S_{Tw\text{-}\lambda}$ (const α)
$S_{Tw\text{-}\alpha}$ (const λ)
a
b
c
d
e
f
g
h
i
j
k
l
(λ↑, α↓)−(λ↓, α↑)
(Tw↑, λ↓)−(Tw↓, λ↑)
(Tw↑,α↓)−(Tw↓,α↑)
Rainfall frequency (event/day)
Rainfall intensity (mm/event)
Rainy season length (days)
Mean Annual Precipitation (mm/year)

Figure 5. Differences in simulated annual GPP as a function of mean annual precipitation and one of the perturbed rainfall characteristics in all the three experiments (i.e. $S_{\lambda-\alpha}$, $S_{Tw-\lambda}$, $S_{Tw-\alpha}$) in the left column. The right column shows the correspondent standard errors (SE, calculated as $SE = \sigma / \sqrt{n}$, where σ refers to the standard deviation within each bin, n is the sample size in each bin, and n and σ are shown in Figure S5), with larger values associated with more uncertainties and requires more caution in interpretation. The contours are based on the binned values, with for each 100 mm/year in MAP, each 0.05 event/day in rainfall frequency, each 1 mm/event in rainfall intensity and each 15 day in rainy season length.

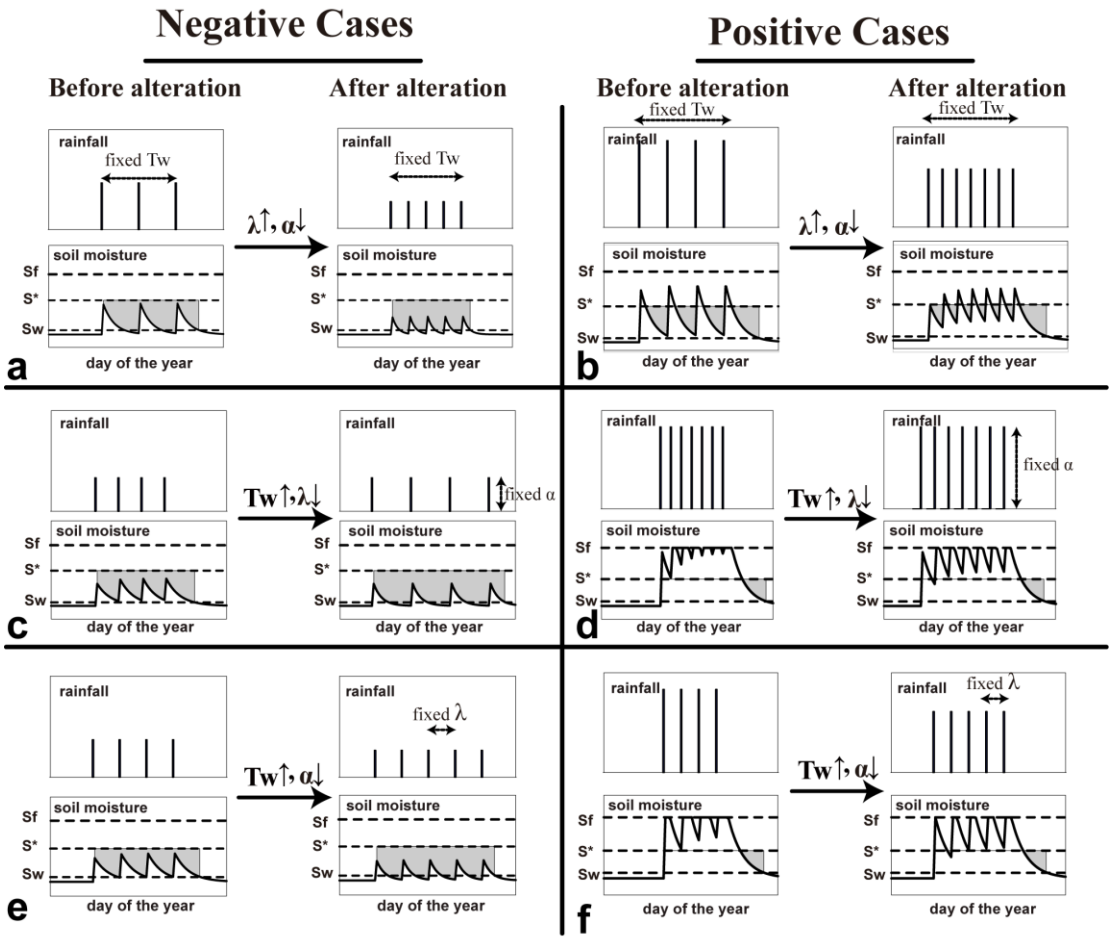

Figure 6. Illustrative time series for hydrological controls on plant root-zone soil moisture dynamics for all the experiments, and these illustrations are generalized based on the simulated time series from the experiments. Both negative and positive cases are shown, and cases with directly hydrological controls are shown (i.e. cloud-induced negative impacts in tropical forests are not shown). The cumulative shaded areas refer to "plant water stress" defined by Porporato et al. (2001).

Supplementary materials:

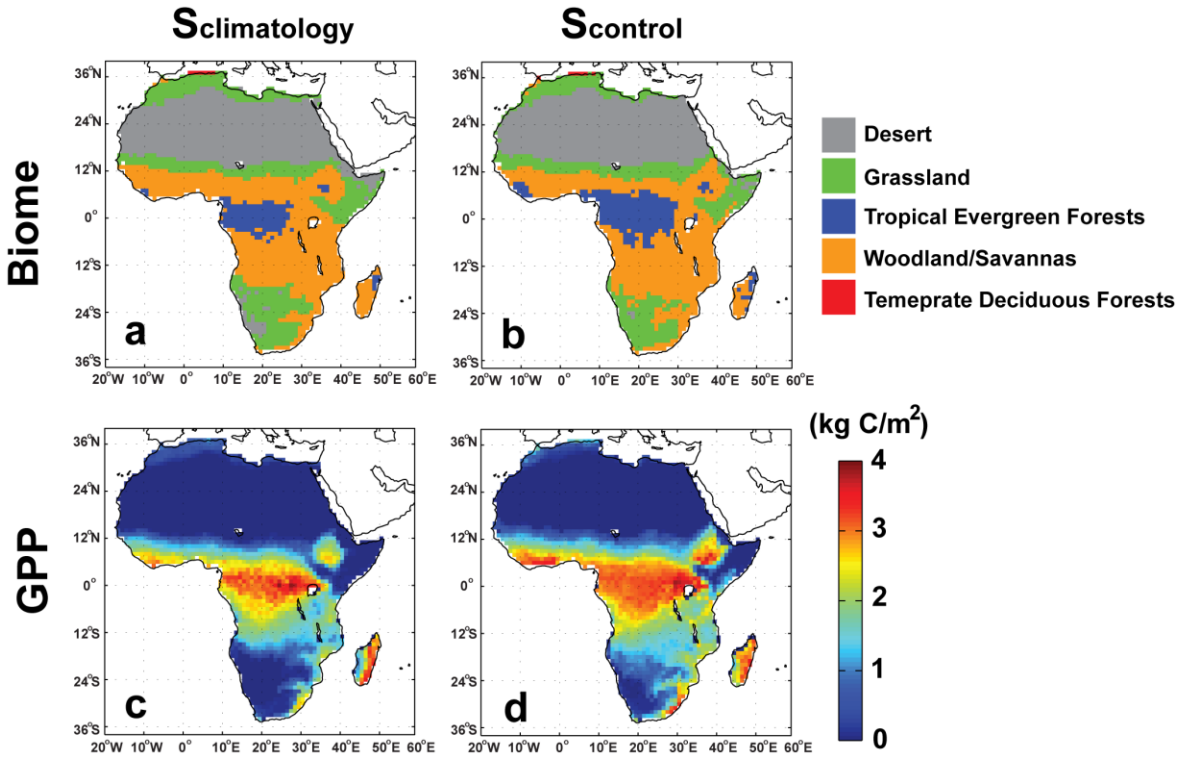

Figure S1. Comparison of biomes and annual GPP between $S_{climatology}$ and $S_{control}$ to test the validity of the synthetic weather generator. The biome definition follows Sato and Ise (2012).

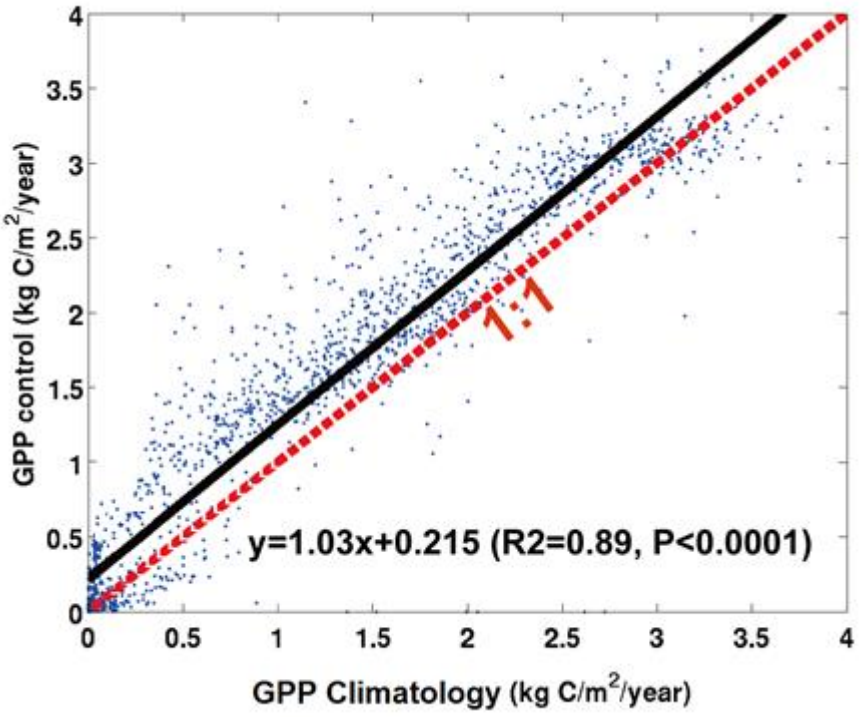

Figure S2. Comparison of simulated annual mean GPP using SEIB-DGVM in the $S_{climatology}$ and $S_{control}$ runs.

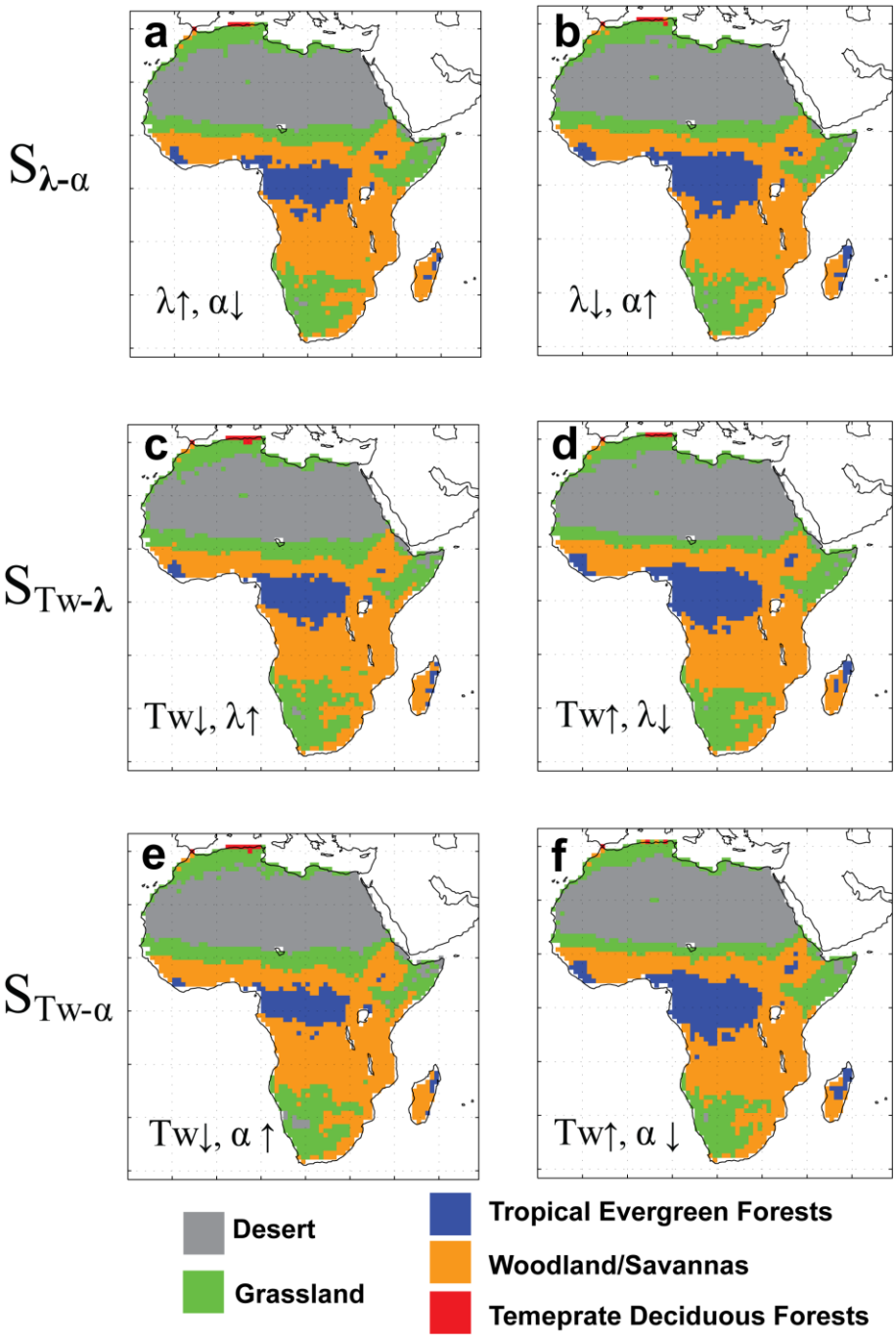

Figure S3. Simulated biomes for different experiments.

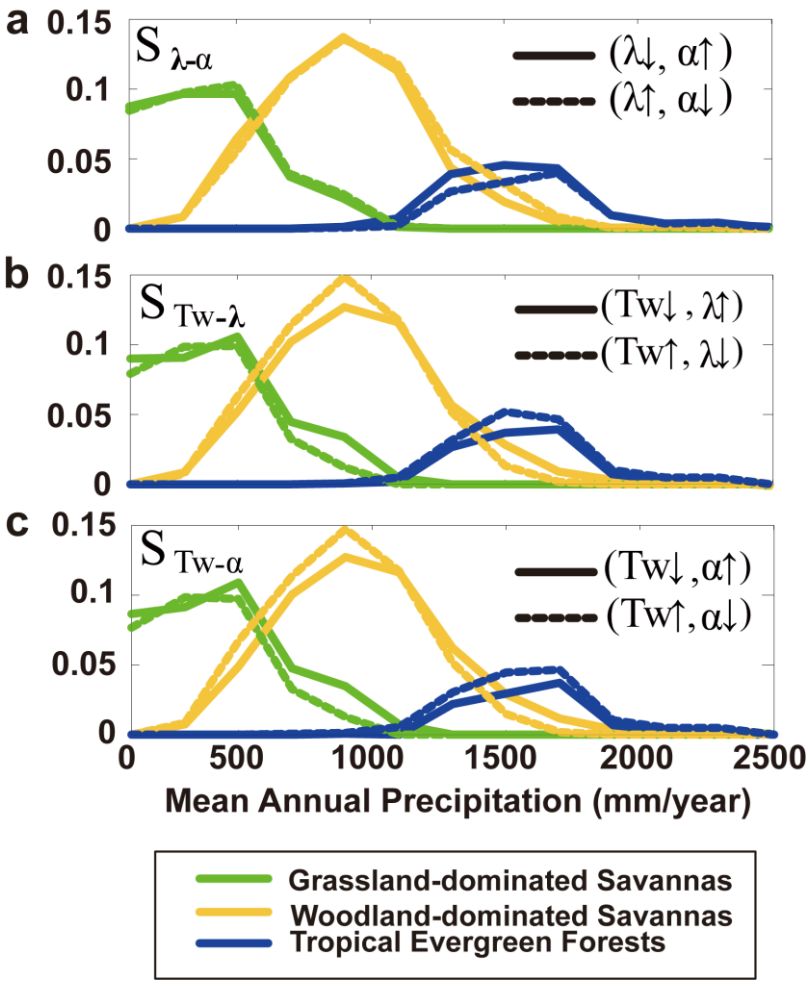

Figure S4. Normalized histograms of three simulated dominating biomes in the three experiments.

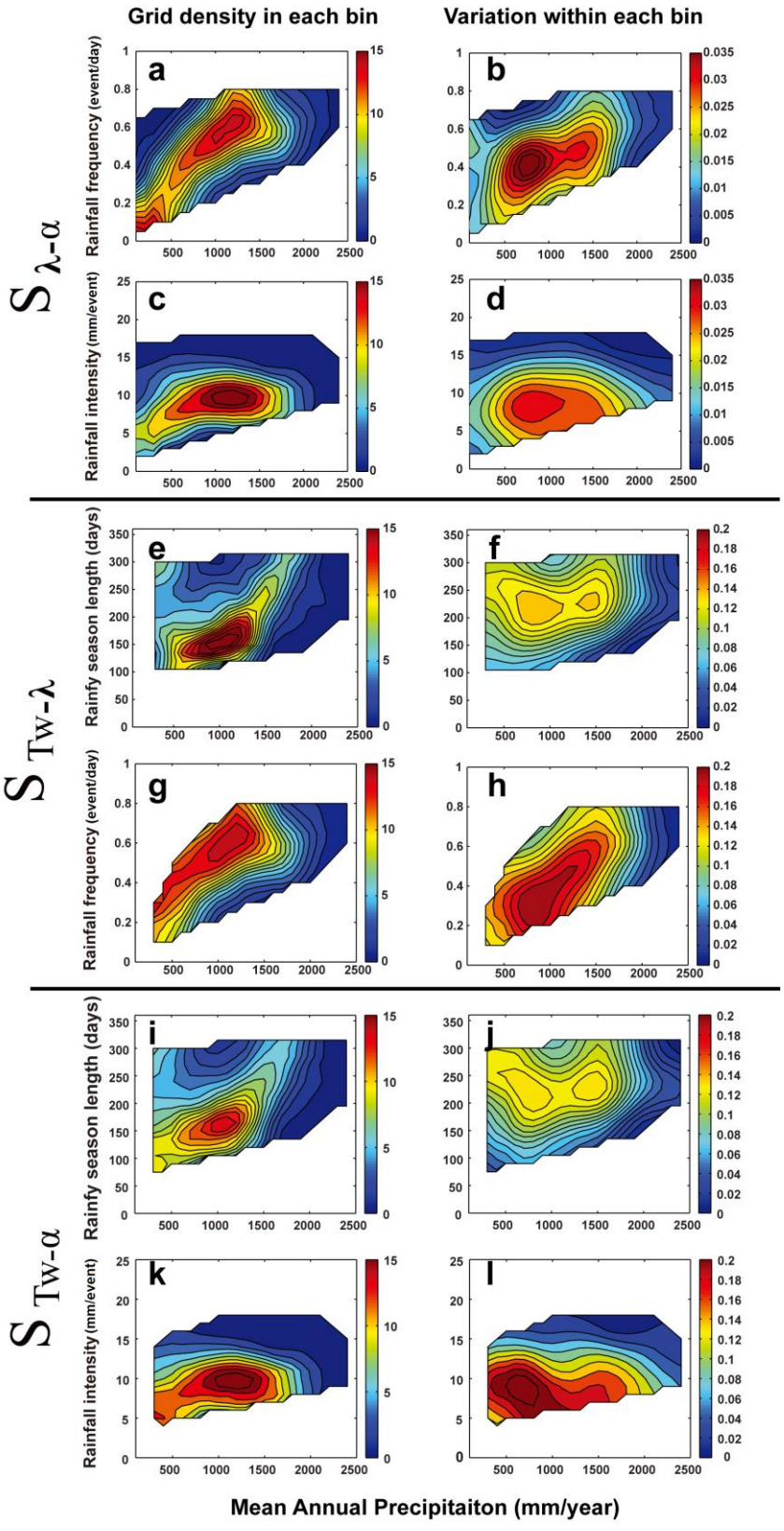

Figure S5. The sample size (n) in each bin (left column) and standard deviation (σ) in each bin (right column), corresponding to Figure 5. In Figure 5 right column, standard deviation (SE) is calculated as $SE = \sigma / \sqrt{n}$.